RESEARCH ARTICLE OPEN ACCESS

Growth and Characterization of Zinc–Magnesium Tris(Thiourea) Sulphate (ZMTS) Single Crystals

A. Darlin Mary [a], K. Jayakumari [b], C.K. Mahadevan[c]
[a] *Department of Physics, Annai Velankanni College,Tholayavattam-629174, Tamil Nadu, India*
[b] *Department of Physics, Sree Ayyappa College for Women, Chunkankadai-629174,Tamil Nadu, India*
[c] *Department of Physics, S.T. Hindu College , Nagercoil-629002, Tamil Nadu, India*

ABSTRACT
Zinc Tris(Thiourea) Sulphate (ZTS) is a semiorganic nonlinear material in the field of photonics and optoelectronics. Single crystals of pure and Magnesium Sulphate mixed Zinc Tris (Thiourea) Sulphate (ZMTS) were grown from aqueous solutions by the slow evaporation method. . The cell parameters of the grown crystals were estimated by single crystal X-ray diffraction technique. The powder X-ray diffraction patterns were recorded and indexed for further confirmation of crystalline nature of grown crystals. The presence of functional groups has been confirmed by FTIR analysis. The FTIR spectrum was recorded in the wavenumber range 400-4000cm^{-1}. The degree of dopant inclusion was ascertained by AAS. The UV-Vis transmittance spectra have been recorded to find the cut-off wavelength. The TGA/DTA studies show the thermal behavior of the grown crystals. The mechanical property of grown crystals has been analyzed by Vicker's microhardness measurement. The nonlinear optical (NLO) property of the grown crystal has been confirmed by Kurtz powder second harmonic generation (SHG) test. The densities of the grown crystals were also measured.
Keywords: ZTS crystals, Doping, Single crystal, Solution growth, Characterization, NLO material.

I. Introduction

In recent years several studies dealing with organic, inorganic and semi organic molecules and materials called nonlinear optics (NLO) are being reported due to the increasing need for photonics applications. The nonlinear (NLO) responses induced in various molecules in solution and solids are of great interest in many fields of research [1,6]. Inorganic and semi organic nonlinear optical (NLO) materials have higher optical quality, larger nonlinearity, good mechanical hardness and low angular sensitivity when compared to organic NLO materials [2]. Zinc Tris (Thiourea) Sulphate (ZTS), $Zn[CS(NH_2)_2]_3SO_4$ is one of the semiorganic nonlinear materials for type II second harmonic generation (SHG)[3,4]. Thiourea molecules are an interesting inorganic matrix modifier due to its large dipole moment and its ability to form an extensive network of hydrogen bonds [7]. The nonlinear optical properties of some of the complexes of thiourea, such as bis(thiourea) cadmium chloride(BTCC), Tris(thiourea) zinc sulphate(ZTS), Tris(thiourea) Magnesium sulphate (MTS) [8], Tris(thiourea) cadmium sulphate (CTS), potassium thiourea bromide (PTB) have gained significant attention in the last few years[9], because both organic and inorganic components in them contribute specifically to the process of second harmonic generation. Nucleation kinetic studies of ZTS crystals have been reported by Ushasree et al.[10]. The centrosymmetric thiourea molecule, when combined with inorganic salt yields noncentrosymmetric complexes, which have the nonlinear optical properties [11].

Two types of semi organic material include organic and inorganic salts and metal organic coordination complexes [12-15]. Zinc Tris(thiourea) sulphate is a good nonlinear optical semi organic material for second harmonic generation. ZTS is 1.2 times more nonlinear than KDP [16]. ZTS possesses orthorhombic structure with $Pca2_1$ space group (point group mm2)[17]. The growth and various studies of doped and undoped ZTS crystals have been reported in a number of publications [18-22]. In this paper we report the results of our work on the growth of pure and Magnesium Sulphate mixed ZTS crystal along with the characterization by X-ray diffraction (XRD), TG-DTA analysis, UV-Visible study, AAS, FT-IR, Microhardness and density.

II. EXPERIMENTAL

The ZMTS salt was synthesized by the stoichiometric incorporation of Analytical Reagent (AR) grade zinc sulphate heptahydrate + magnesium sulphate heptahydrate and thiourea in the molar ratio 1:3. The component salts were very well dissolved in deionized water, which was thoroughly mixed using a magnetic stirrer and the mixture was heated at 50°C till a white crystalline salt of ZMTS was obtained. Temperature was maintained at 50°C to avoid decomposition. ZMTS salt was synthesized according to the reaction.

$Zn_xMg_{1-x}SO_4 .7H_2O + 3CS(NH_2)_2 \rightarrow Zn_xMg_{1-x}[(CS(NH_2)_2)_3]SO_4$
where x=0.0 to 1 in steps of 0.1

Single crystals of ZMTS were grown by solution growth employing the slow evaporation technique at room temperature (31°C). Transparent and colorless ZMTS crystals of size 7x7x4 mm^3 were harvested in 20-25 days except MTS crystal. The MTS crystal of size 9x8x5 mm^3 was white in color and harvested in 30-35 days.

The grown single crystals of pure and ZMTS crystals were subjected to single crystal XRD analysis using an ENRAF NONIUS CAD4 diffractometer with MoK_α radiation (λ = 0.71073 Å) to determine unit cell dimensions [thanks to IIT, Chennai].

The powder X-ray diffraction (XRD) patterns were obtained using a powder X-ray diffractometer. [Model: Ritz-170 with Nickel filtered CuK_α radiation (1.54056 Å).

The Infrared spectroscopy is effectively used to identify the functional groups to determine the molecular structure of the grown crystals. The FT-IR spectra of the samples were recorded using a Perkin Elmer Lambda 35 IR spectrophotometer by KBr pellet technique in the wavenumber range 400-4000 cm^{-1}.

The optical transmission spectrum was recorded using Perkin Elmer Lambda 35 spectrophotometer in the wavelength region 190– 1100 nm. The Second Harmonic Generation (SHG) test for the grown ZMTS crystals were performed by the powder technique of Kurtz and Perry [30] using a pulsed Nd:YAG laser (λ = 1064 nm).

Atomic absorption studies of Magnesium Sulphate mixed ZTS crystals were carried out using an atomic absorption spectrometer (Model: AA 6300).

Thermal analysis was carried out using Perkin-Elmer DTA/TGA analyzer in the air atmosphere. The thermo gravimetric analysis (TGA) and differential thermal analysis (DTA) were carried out for a sample in the temperature range 40 - 730°C at a heating rate of 20°C/min in air atmosphere.

The Micro hardness of the grown crystals was measured using Shimadzu HMV- 2 micro hardness tester.

The flotation method was employed for the precise determination of density and this method is sensitive to point defects and insensitive to dislocation of crystals unlike other methods of density measurements [23]. Bromoform (density: 2.896g/cc) and carbon tetrachloride (density: 1.594 g/cc) were used as high and low density liquids respectively.

III. RESULTS AND DISCUSSION

3.1 X-ray diffraction analysis

The grown ZMTS ($Zn_xMg_{1-x}[(CS(NH_2)_2)_3]SO_4$ where x=0.0 to 1 in steps of 0.1) crystals are displayed in Fig. 1. The external appearance of the grown crystals is found to be different when Magnesium content increases. The Lattice parameter values of the grown ZMTS crystals were shown in Table 1. It shows that the grown pure ZTS and $Zn_xMg_{1-x}[(CS(NH_2)_2)_3]SO_4$ crystals belong to orthorhombic system. The MTS crystal belongs to monoclinic system. The space group and number of molecules per unit cell for both the grown crystals were found to be $Pca2_1$ and 4,2 respectively, and they are in good agreement with the reported values [24].

The powder XRD patterns of ZMTS crystals are shown in Fig. 2. Sharp peaks of powder XRD spectrum of the crystal show good crystalline nature of the Compound. Lattice parameter of the pure crystal coincides well with the reported values. There is only slight variation in the grown crystals in powder form were indexed using the TREOR software package following the procedure of Lipson and steeple [26]. Also UNITCELL software package was used to confirm the indexing.

Table 1: Lattice parameter values of the grown ZMTS

Sample	a (Å)	b (Å)	c (Å)	V ($Å^3$)	Angle	Structure
ZTS	7.77 [7.72]	11.11 [11.11]	15.48 [15.47]	1340 1340]	α=β =γ =90°	Ortho rhombic
ZTS9	7.78	11.12	15.47	1341	α=β =γ =90°	"
ZTS8	7.77	11.13	15.46	1339	α=β =γ =90°	"
ZTS7	7.76	11.14	15.45	1338	α=β =γ =90°	"
ZTS6	7.75	11.15	15.48	1337	α=β =γ =90°	"
ZTS5	7.77	11.14	15.47	1340	α=β =γ =90°	"
ZTS4	7.78	11.13	15.46	1338	α=β =γ =90°	"
ZTS3	7.77	11.12	15.45	1337	α=β =γ =90°	"
ZTS2	7.76	11.11	15.44	1339	α=β =γ =90°	"
ZTS1	7.74	11.08	15.42	1337	α=β =γ =90°	"
MTS	7.66 [7.67]	5.49 [5.48]	8.55 [8.56]	359 [360]	α =γ =90°, β=138. 11	Mono clinic

Reported values are given in parenthesis [27, 8]

Figure 1. Photograph showing sample crystals.
(**Top row**: from left are ZTS1 – $Zn_{0.1}Mg_{0.9}$ [(CS $(NH_2)_2)_3$] SO_4 ZTS2 – $Zn_{0.2}Mg_{0.8}$ [(CS $(NH_2)_2)_3$] SO_4 , ZTS3 – $Zn_{0.3}Mg_{0.7}$ [(CS $(NH_2)_2)_3$] SO_4 , ZTS4 – $Zn_{0.4}Mg_{0.6}$ [(CS $(NH_2)_2)_3$] SO_4 , ZTS5 – $Zn_{0.5}Mg_{0.5}$ [(CS $(NH_2)_2)_3$] SO_4 ,
and **middle row**: from left are ZTS6 – $Zn_{0.6}Mg_{0.4}$ [(CS $(NH_2)_2)_3$] SO_4 , ZTS7 – $Zn_{0.7}Mg_{0.3}$ [(CS $(NH_2)_2)_3$] SO_4 , ZTS8 – $Zn_{0.8}Mg_{0.2}$ [(CS $(NH_2)_2)_3$] SO_4 , ZTS9 – $Zn_{0.9}Mg_{0.1}$ [(CS $(NH_2)_2)_3$] SO_4 ,
and **bottom row**: from left are ZTS – Zn_1Mg_0 [(CS $(NH_2)_2)_3$] SO_4, MTS – Zn_0 Mg_1 [(CS $(NH_2)_2)_3$] SO_4

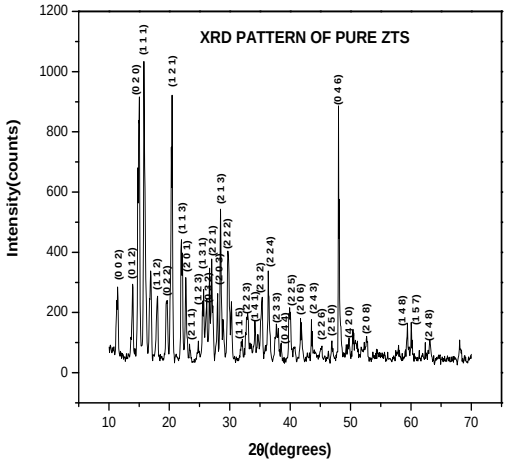

a)

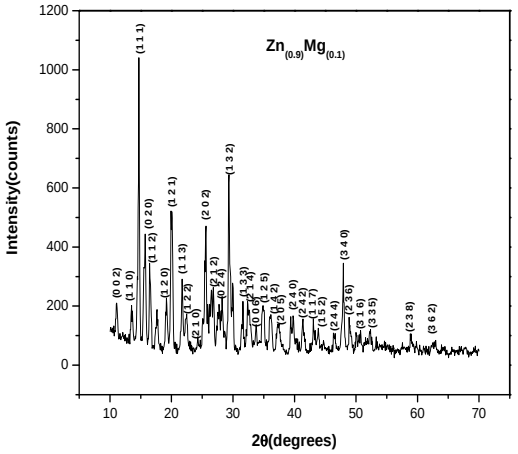

b)

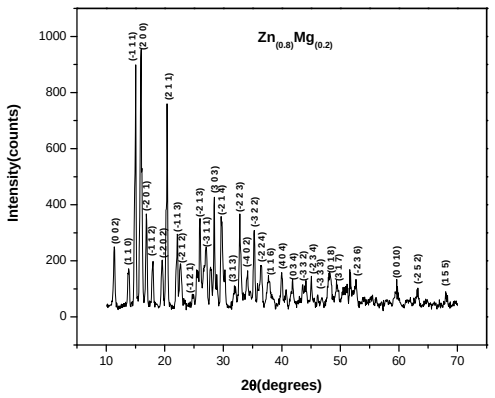

c)

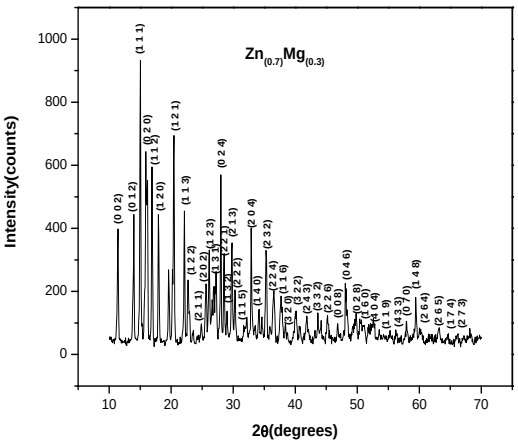

d)

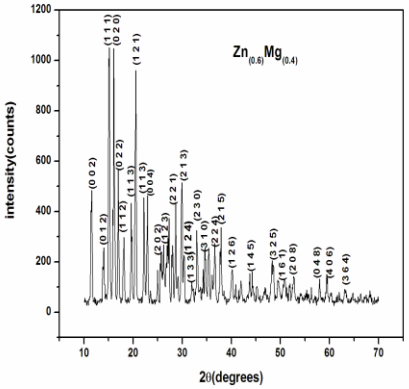
Zn(0.6)Mg(0.4)
intensity(counts)
2θ(degrees)

e)

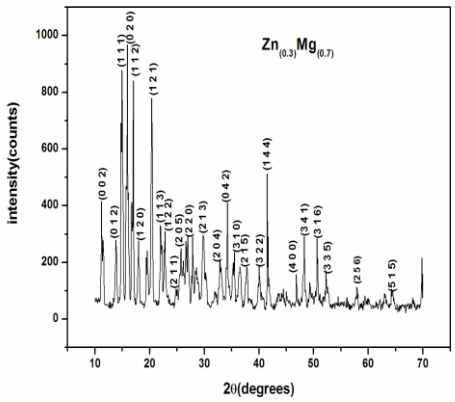
Zn(0.3)Mg(0.7)
intensity(counts)
2θ(degrees)

h)

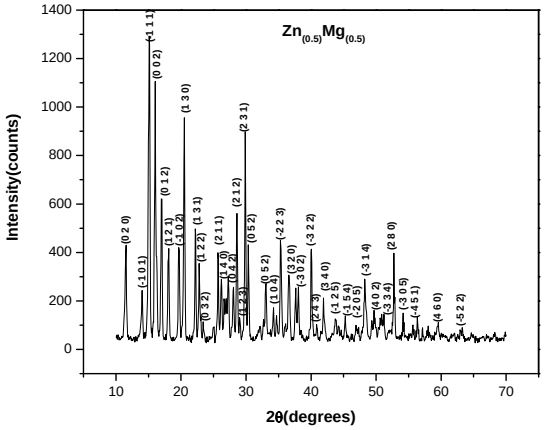
Zn(0.5)Mg(0.5)
Intensity(counts)
2θ(degrees)

f)

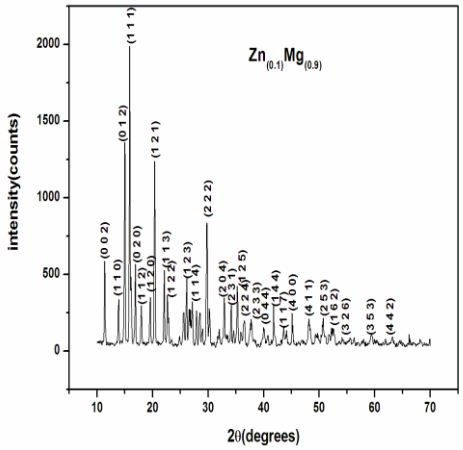
Zn(0.1)Mg(0.9)
intensity(counts)
2θ(degrees)

i)

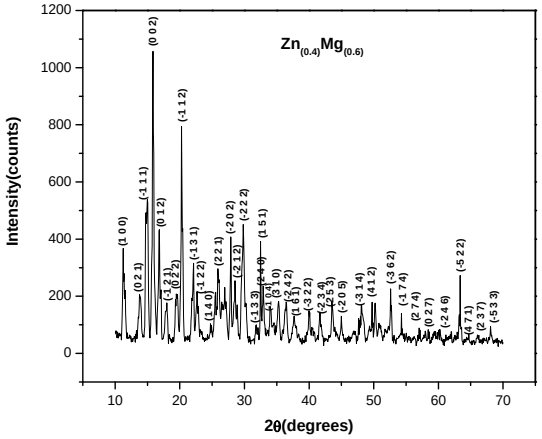
Zn(0.4)Mg(0.6)
Intensity(counts)
2θ(degrees)

g)

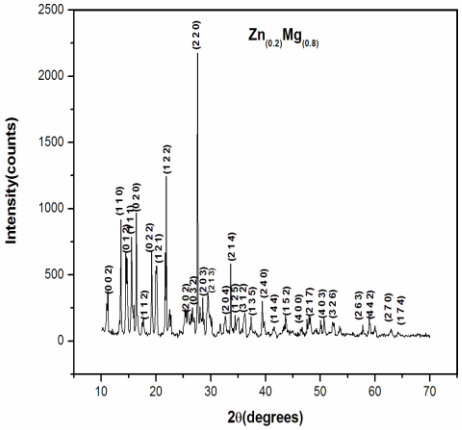
Zn(0.2)Mg(0.8)
Intensity(counts)
2θ(degrees)

j)

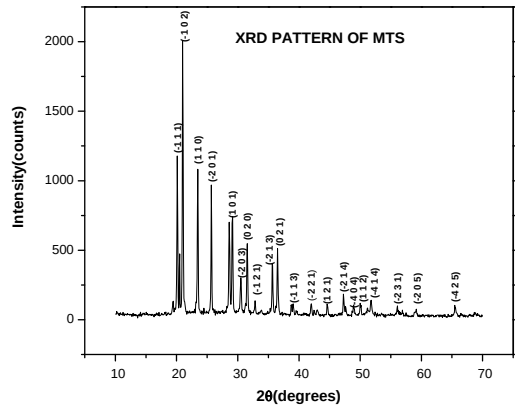

k)

Figure 2: The PXRD patterns obtained for the ZMTS crystals
(a) ZTS b) ZTS9 (c) ZTS8 (d) ZTS7 (e) ZTS6 (f) ZTS5 (g)ZTS4 (h) ZTS3 (i) ZTS2 (j) ZTS1 (k) MTS

3.2 FT-IR analysis

The FTIR spectra of the samples were recorded using a Perkin – Elmer spectrum FT-IR spectrometer by the KBr pallet technique in the wave number range **400-4000** cm^{-1} in order to confirm the presence of functional groups. The recorded FT-IR spectrum of ZMTS crystals are shown in Fig. 3. In ZTS compound, there are three thiourea groups and one sulphate ion. Each thiourea group consists of one carbon atom bonding to one sulfur and two nitrogen atoms. Each of the nitrogen atoms in thiourea is connected to two hydrogen atoms. Zinc ion is tetrahedrally coordinated to three sulfur atoms of thiourea and to an oxygen atom of sulfate ion [5]. The spectra of ZMTS crystals can be interpreted as follows: The N-H absorption band at higher frequency region between 3000 and 4000 cm^{-1} arises due to symmetric and asymmetric vibration of NH_2 group of the zinc coordinated thiourea. The bending vibration of NH_2 was observed at around 1627 cm^{-1} .

The symmetric N-C-N stretching vibration are observed near 1510 cm^{-1}.The absorption band at 1405 cm^{-1} assigned to the C=S asymmetric stretching vibration. In pure thiourea, C= S is bonded to NH_2, whereas in mixed crystals it is bonded to metal ions and therefore the C=S stretching vibration is also shifted to lower values from 730 to 713 cm^{-1} and this shifting of C= S stretching frequency confirms the coordination of metal- sulphur bond [31].The symmetric bending vibration of N-C-N was observed near 474 cm^{-1}. The asymmetric bending vibration of NH_2 was observed near 590 cm^{-1} .The presence of peaks near 1000cm^{-1} confirms the presence of sulfate ion in the coordination sphere. When ZTS is mixed with different concentrations of Magnesium more NH stretch vibrations are introduced due to mixing and as a result the NH absorption peak becomes stronger.

Table 3 : Comparison of IR bands of MTS with thiourea and ZTS
(*υ_{as}-asymmetric stretching, υ_s-symmetric stretching, δ_{as}-asymmetric bending, ρ- rocking, δ-bending, δ_s- symmetric bending*)

Thiourea **cm^{-1}**	ZTS [29] **cm^{-1}**	ZTS Present Work **cm^{-1}**	MTS [8] **cm^{-1}**	MTS Present work **cm^{-1}**	Assign ments
3376	3378	3367	3368	3380	$\upsilon_{as}(NH_2)$
3280	3206	3208	3298	3276	$\upsilon_{as}(NH_2)$
3167	3206	3177	-	3176	$\upsilon_s(NH_2)$
1627	1633	1631	1611	1616	$\delta_{as}(NH_2)$
-	1496	1512	1472	-	υ_s(N-C-N)
1417	1404	1401	1413	1411	υ_{as}(C=S)
1089	1126	1147	1084	1080	ρ(NH2)
740	717	714	730	727	υ_s(C=S)
469	508	593	-	628	δ(NH2)
411	424	471	431	-	δ_s(N-C-N)

Table 2: Comparison of IR bands of ZMTS crystals
(*υ_{as}-asymmetric stretching, υ_s-symmetric stretching, δ_{as}-asymmetric bending, ρ- rocking, δ-bending, δ_s-symmetric bending*)

ZTS (cm^{-1})	ZTS9 (cm^{-1})	ZTS8 (cm^{-1})	ZTS7 (cm^{-1})	ZTS6 (cm^{-1})	ZTS5 (cm^{-1})	ZTS4 (cm^{-1})	ZTS3 (cm^{-1})	ZTS2 (cm^{-1})	ZTS1 (cm^{-1})	MTS (cm^{-1})	Assignments
3367	3368	3368	3369	3368	3371	3369	3368	3360	3369	3380	$\upsilon_{as}(NH_2)$
3308	3297	3308	3293	3309	3297	3308	3308	-	-	3276	$\upsilon_{as}(NH_2)$
3177	3191	3192	3181	3181	3186	3189	3172	3189	3194	3176	$\upsilon_s(NH_2)$
2711	2714	2714	2704	2713	2704	2712	2713	2711	2713	2679	O-H stretching
1631	1632	1631	1633	1632	1633	1632	1633	1631	1632	1616	$\delta_{as}(NH_2)$
1512	1512	1512	1513	1512	1512	1512	1513	1516	1513	-	υ_s(N-C-N)
1401	1402	1402	1402	1403	1402	1402	1402	1403	1402	1411	υ_{as}(C=S)
1147	1148	1147	1148	1148	1149	1147	1148	1153	1148	-	$\rho(NH_2)$
1030	1031	1031	1031	1031	1031	1032	1031	1032	1031	-	$\rho(NH_2)$
950	950	951	950	951	950	951	950	955	951	1080	C-H (out of plane)
714	714	714	714	714	714	714	714	717	714	727	υ_s(C=S)
593	595	596	595	595	595	596	595	526	596	628	$\delta(NH_2)$
471	474	474	472	473	474	474	474	474	474	-	δs(N-C-N)

Table 4 : Lower cut off wavelength and band gap energy of ZMTS crystals

Sample	**Lower cut off wavelength (nm)**	**Band gap energy (ev)**
ZTS	290[35]	4.264[36]
ZTS9	280	4.419
ZTS8	240	5.156
ZTS7	238	5.199
ZTS6	236	5.24
ZTS5	275	4.5
ZTS4	278	4.45
ZTS3	234	5.288
ZTS2	207	5.978
ZTS1	201	6.156
MTS	300[8]	4.125

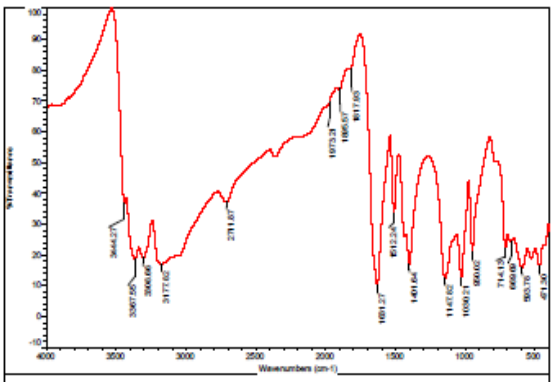

a)

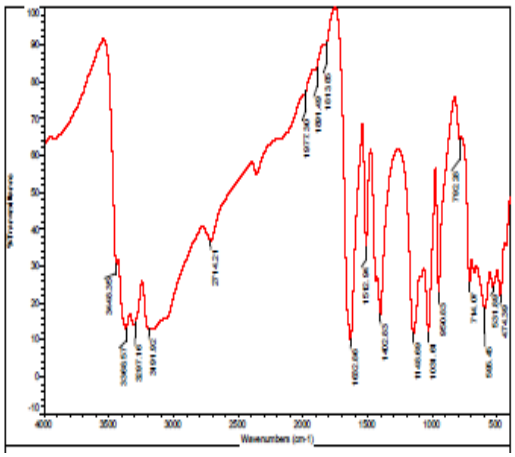

b)

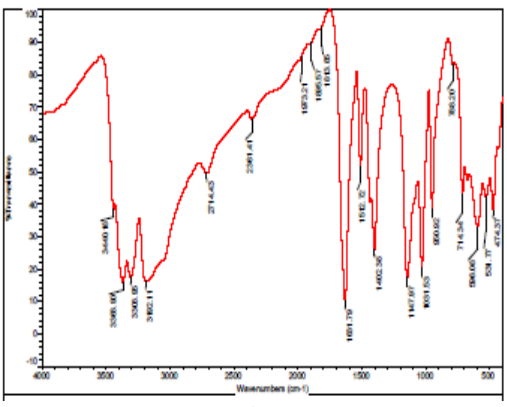

c)

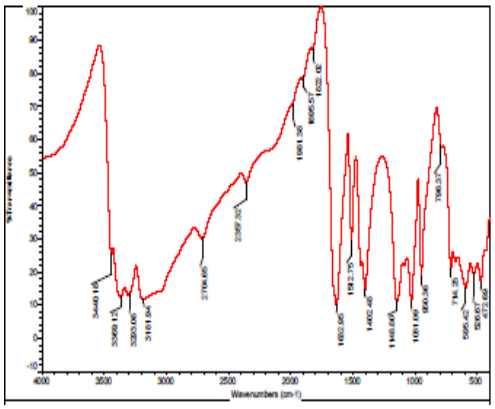

d)

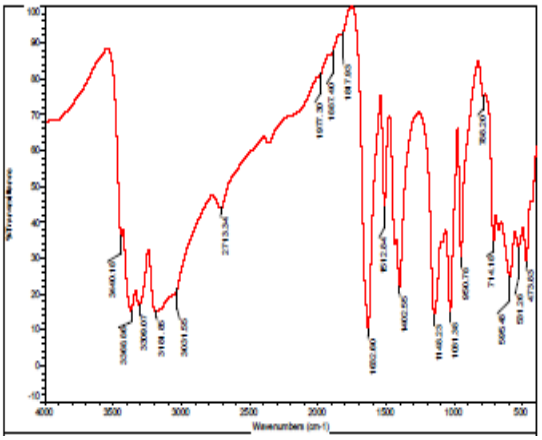

e)

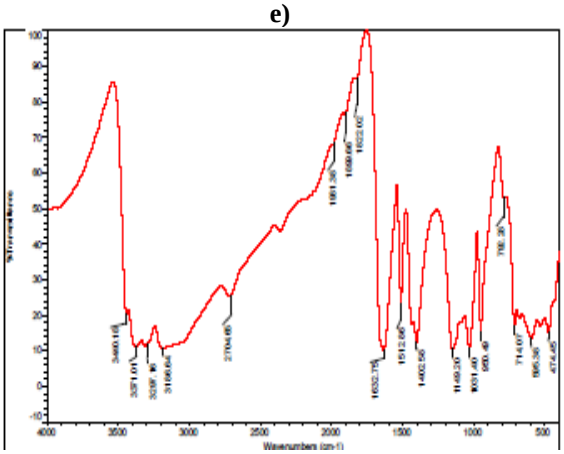

f)

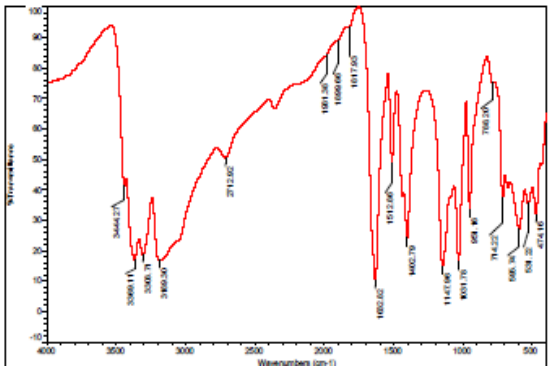

g)

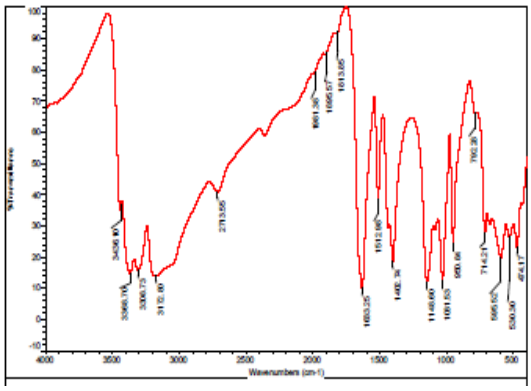

h)

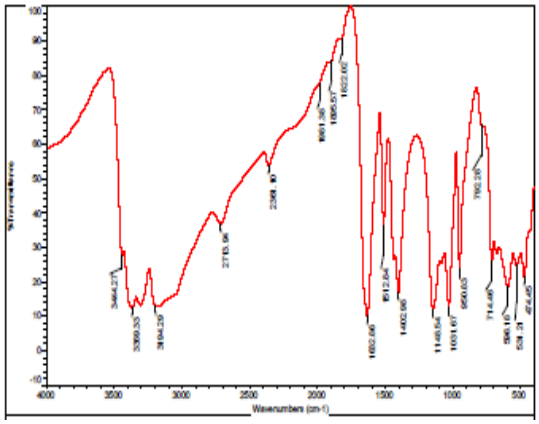

i)

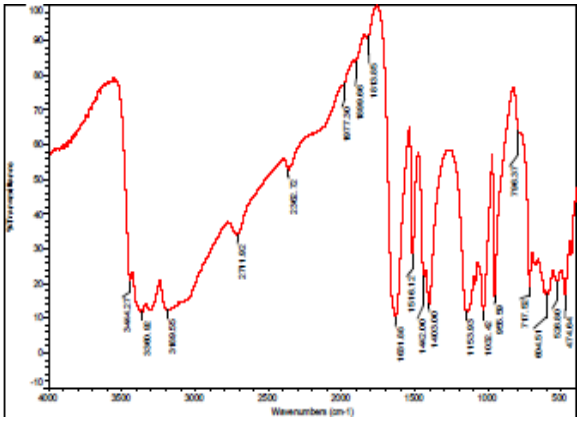

j)

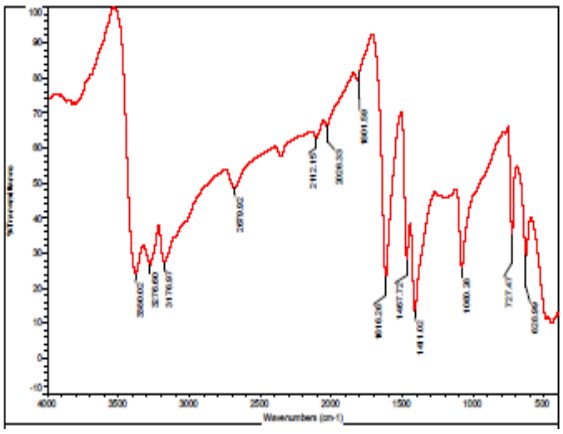

K)

Figure 3: (a) ZTS b) ZTS9 (c) ZTS8 (d)ZTS7 e) ZTS6 (f) ZTS5 (g)ZTS4 (h) ZTS3 (i)ZTS2 (j)ZTS1 (k)MTS

3.3 UV–Visible spectral analysis

The single crystals are mainly used for optical applications. Thus the study of optical transmission range of grown crystal is important. The optical transmission spectrum was recorded using Perkin Elmer Lambda 35 spectrophotometer in the wavelength region 190– 1100 nm. The transmittance spectra show the grown crystals have lower cutoff wavelengths at around 290nm for ZTS crystal. The grown ZMTS crystal has good transmission in UV as well as in visible regions, it is shown in Fig.4. The wide range of transparency in UV, visible and IR regions enables good transmission of the second harmonic frequency of Nd:YAG laser. The forbidden band gap for the grown crystals of this work was calculated using the relation E=hc/λ, where 'h' is the Planck's constant, 'c' is the velocity of light and 'λ' is the cut-off wavelength. The obtained value for the forbidden gap for all crystals was shown in Table4. From UV-Visible data we have plotted a graph of absorbance vs. photon energy in ev and from that graph it can be concluded that band gap is direct type [37]. Thus grown crystal has good transmission in UV as well as in visible region. This is an added advantage in the field of optoelectronic applications. The band gap and lower cut off wavelength are shown in Table 4.

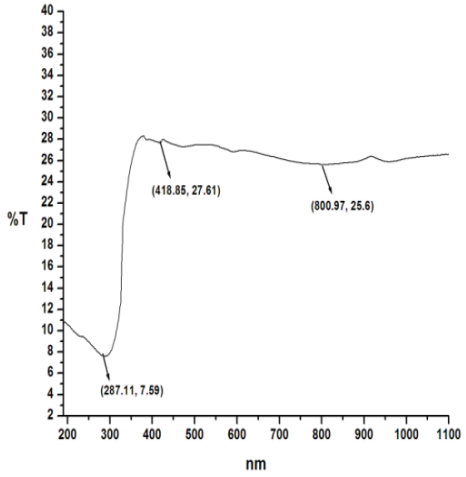
%T
nm
(418.85, 27.61)
(800.97, 25.6)
(287.11, 7.59)

a)

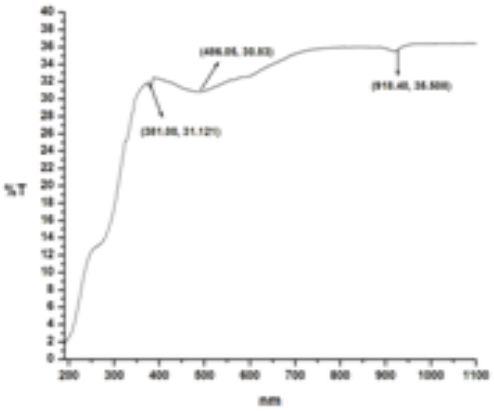
%T
nm

b)

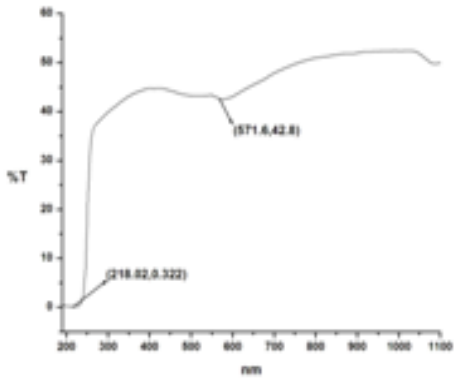
%T
nm
(571.6,42.8)
(218.82,0.322)

c)

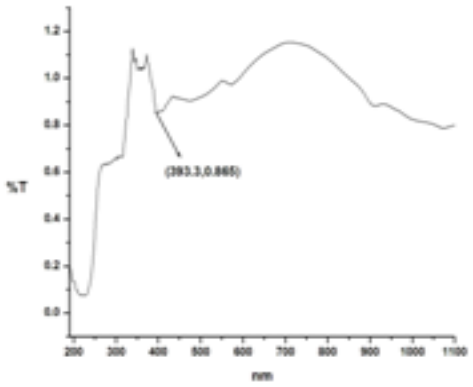
%T
nm
(393.3,0.865)

d)

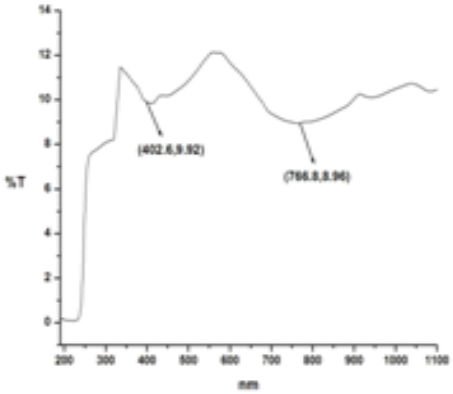
%T
nm
(402.6,9.92)
(766.8,8.96)

e)

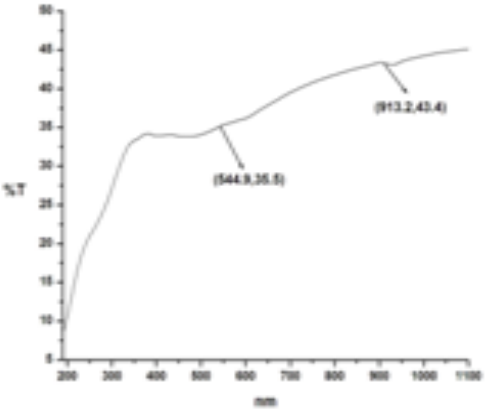
%T
nm
(913.2,43.4)
(544.9,35.5)

f)

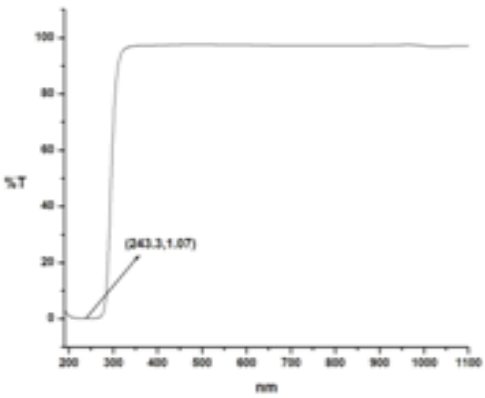
%T
nm
(243.3,1.07)

g)

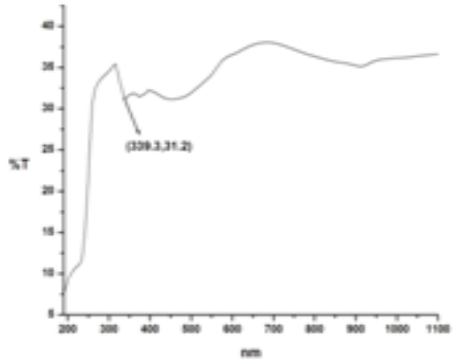

h)

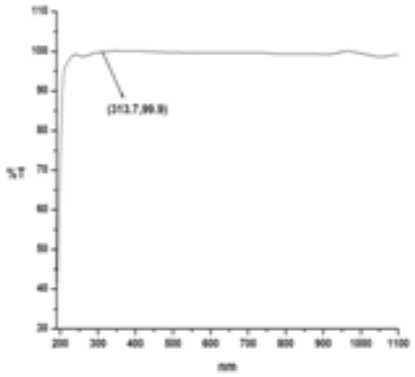

i)

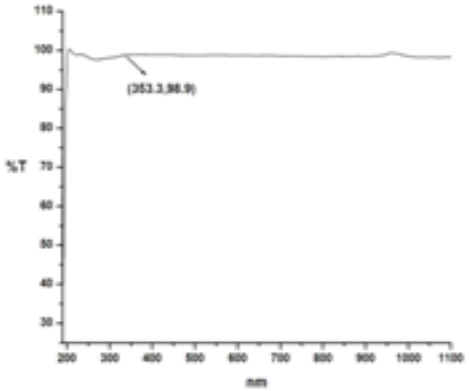

j)

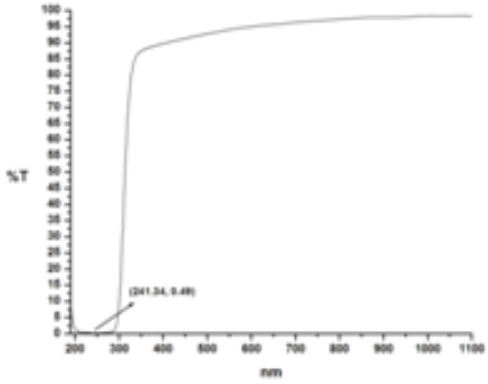

k)

Figure 4: Transmittance spectrum of ZMTS crystals

(a) ZTS b) ZTS9 (c) ZTS8 (d)ZTS7 (e) ZTS6 (f)ZTS5 (g)ZTS4 (h) ZTS3 (i) ZTS2 (j)ZTS1 (k) MTS

3.4 Second harmonic generation (SHG) efficiency

The second harmonic generation (SHG) conversion efficiency of ZMTS was measured by Kurtz and Perry powder technique [30]. The crystal was grounded into a fine powder and densely packed between two transparent glass slides. A Q switched Nd: YAG laser emitting a fundamental wavelength of 1064 nm (pulse width 8 ns) was allowed to strike the sample cell. The SHG output 532nm (green light) was finally detected by the photomultiplier tube. The powdered material of potassium dihydrogen phosphate (KDP) was used in the same experiment as a reference material. The relative conversion efficiency was calculated from the output power of ZMTS crystals with reference to ZMTS and KDP crystals. The powder SHG efficiency output of pure ZTS was found to be 0.78 times greater with respect to KDP. The Kurtz powder SHG test confirms the NLO property of the grown ZMTS crystals. Second harmonic generation efficiency of ZTMS compared with KDP is shown in Table 5.

Table 5: SHG Conversion of KDP, ZMTS

Output power in milli Joules (mJ)			**Relative conversion efficiency of ZMTS**
Sample	**ZMTS**	**KDP**	**(SHG in %)**
ZTS	6.9	8.8	78.4
ZTS9	6.4		72.7
ZTS8	6.3		71.6
ZTS7	6.2		70.5
ZTS6	5.9		67.0
ZTS5	5.8		65.9
ZTS4	5.7		64.7
ZTS3	4.6		52.3
ZTS2	4.3		48.8
ZTS1	4.2		47.7
MTS	6.6		75.0

3.5 Atomic Absorption Spectroscopy (AAS)

Atomic Absorption Spectroscopy (AAS) is one of the most widely used quantitative analytical methods. AAS is used for quantitative determination of metals and metalloids down to absolute amounts as low as 10^{-14}g. AAS determines the presence of metals in liquid samples. Metals include Fe, Cu, Al, Zn, Mg, Hg, and many more. It also measures the concentrations of metals in the samples. To determine the mole percentage of dopants incorporated in the grown doped crystals, finely powdered and then subjected to AAS. The results of AAS are presented in Table 6. The amount of dopant incorporation was

found to be far below its original concentration in their respective solution. The low percentage of incorporation of dopants into the crystal may be due to large difference between the ionic radii.

The presence of Zn and Mg in the crystals was confirmed by atomic absorption studies. From the AAS study that only a low concentration of Magnesium has entered into the lattice of the ZMTS crystals.

Table 6: Atomic Absorption Spectra Estimate

Sample	atomic % of (Zn)	atomic % of (Mg))
ZTS	16.25	-
ZTS9	15.81	11.12
ZTS8	15.78	12.07
ZTS7	15.62	13.28
ZTS6	15.41	13.15
ZTS5	15.19	19.12
ZTS4	14.85	21.16
ZTS3	13.31	22.14
ZTS2	12.96	23.27
ZTS1	12.27	24.8
MTS	-	44.63

3.6 Mechanical test

Micro hardness test is one of the best methods for understanding the mechanical properties of materials. Hardness of the material is a measure of resistance that offers to deformation. To find surface hardness of the grown ZTMS crystal, micro hardness was measured from 25 g to 100 g load using Shimadzu HMV- 2 micro hardness tester. The transparent polished crystal free from cracks was selected for hardness measurement. Micro hardness studies were carried out at room temperature and the time of indentation is kept constant at 5 sec for all the loads. The hardness of the material H_v was calculated by the relation, $H_v = 1.8544\ P/d^2\ kg/mm^2$. Where P is the applied load and d is the mean diagonal length of the indentation. A graph was plotted for hardness versus load P (Fig. 5(a)) which shows that the hardness increases with the increase of load [28] for ZMTS crystals. The Meyer index number can be calculated from the Meyer's law which relates the load and indentation diagonal length

$P = kd^n$,

$$\text{Log } P = \text{Log } k + n \text{ Log } d$$

Where P is load in kg, d is the diameter of recovered indentation in mm, k is constant and n is the work hardening coefficient. The plots between log P against log d for ZMTS crystals are shown in Fig. 5(b), which give straight lines after least square fit. The slope of the straight lines of the figure gives the work hardening coefficient (n). The n value of ZTS crystal is found to be 3.379 which as in good agreement with the reported value. The obtained values are shown in Table 7. Careful observations of Kishan Rao et al [31] on various materials have pointed out that n lies between 1 and 1.6 for hard materials and it are more than 1.6 for soft materials. According to Onitsch [32], if n is greater than 1.6, the micro hardness number increases with increase in load. Since the obtained values of n for ZMTS crystals are more than 1.6, the grown crystals of this work belong to the category of soft materials and hardness number increases with the load and it is useful for non-linear optical applications.

Table 7: Work hardening coefficient of ZMTS crystals

Sample	Work hardening coefficient (n)
ZTS	3.3793
ZTS9	2.8476
ZTS8	2.7917
ZTS7	3.9353
ZTS6	2.8831
ZTS5	3.2434
ZTS4	3.1437
ZTS3	3.8009
ZTS2	2.9389
ZTS1	4.1138
MTS	4.1486

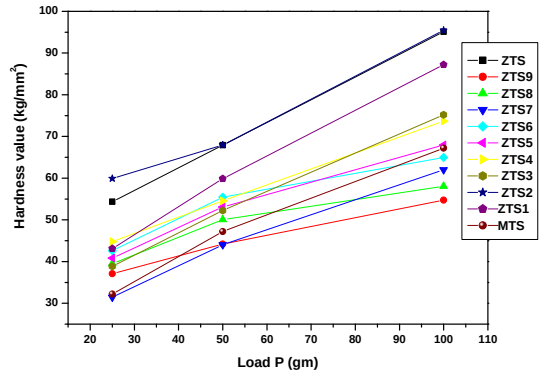

Figure 5(a): Variation of hardness value Vs Load P of ZMTS crystals

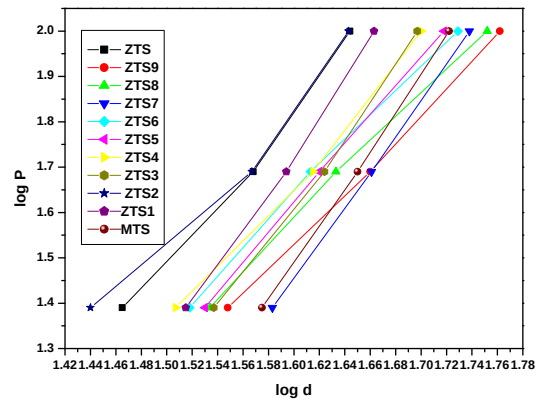

Figure 5(b): Plots of log P Vs log d for ZMTS crystals

3.7 Thermal analysis

The chemical decomposition, phase transition temperature, melting point and the weight loss of the grown crystals were determined by thermo gravimetric analysis. The thermo gravimetric analysis (TGA) was carried out by using Perkin Elmer instruments, Model: Q600 SDT Thermal Analyzer in the temperature range 40.00°C to 730.00°C at a heating rate of 20 °C /min. The experiment was performed in air atmosphere. The thermo grams are shown in Fig. 6. The TGA trace shows the different stages of decomposition. In Fig. 6 (a) ZTS shows, the first endothermic peak in DTA at 242.48 ºC. Further endothermic peaks are observed at 296.05 ºC and 354.90 ºC. The TGA curve shows that the sample undergoes a complete decomposition between 239 ºC and 730 ºC. The weight loss in the temperature range 240 ºC–275 ºC is due to the liberation of volatile substances like sulfur oxide in the compound [33]. The sharpness of this endothermic peak shows the good degree of crystallinity and purity of the sample. In the ZTS, a weight loss about 75 % [34] occurs at 730 ºC. When Magnesium is added with ZTS, the melting point of ZTS is increasing and decreasing slightly. When compared to pure ZTS, the MTS melting point is greater. The melting point of MTS is found to be at 181.40 ºC. There is no major weight loss up to 181 ºC. So the crystal is thermally stable up to 181ºC. It is observed that there is maximum weight loss in the temperature range 181.40 ºC–233.21 ºC compared with subsequent stages. It concludes that the thermal stability of ZTS decreasing with adding different concentration of Magnesium. There is no phase transition till the material melts, this increases the temperature range for the use of crystal in NLO application. The absence of water in molecular structure is confirmed by the absence of weight loss around 100 ºC. There is no decomposition up to melting point; this ensures thermal stability of material for lasers. Fig. 6 shows TGA-DTA curves of ZMTS crystals.

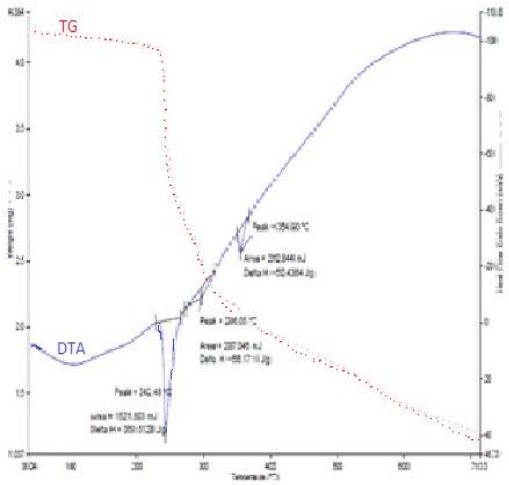

a)

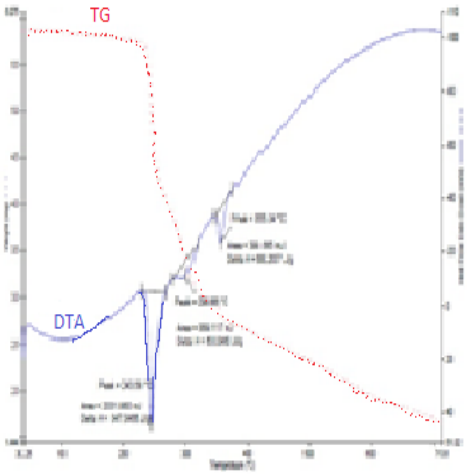

b)

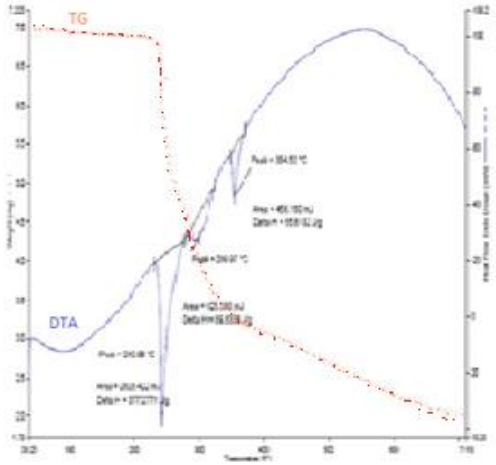

c)

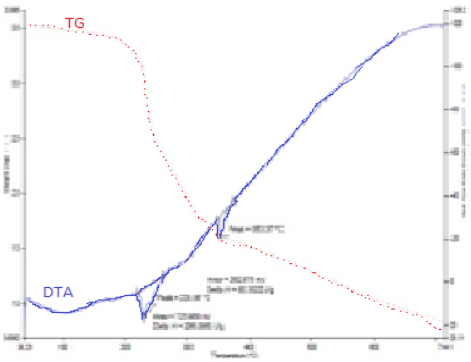

f)

Figure 6: TGA-DTA curve of ZMTS crystals. (a) ZTS b) ZTS9 (c) ZTS8 (d)ZTS7 (e) ZTS6 (f)ZTS5 (g)ZTS4 (h) ZTS3 (i)ZTS2 (j)ZTS1 (k)MTS

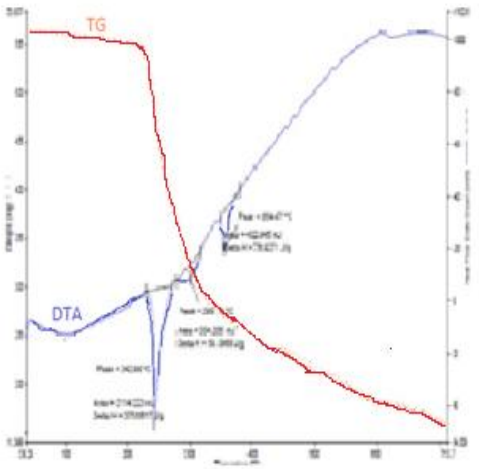

d)

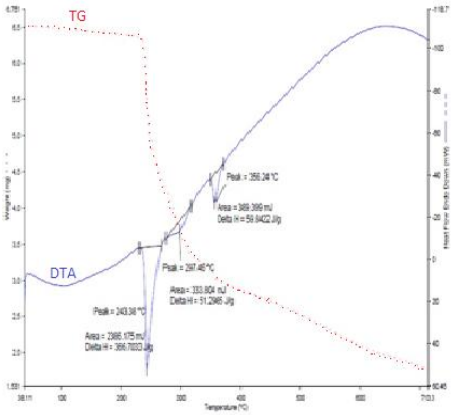

g)

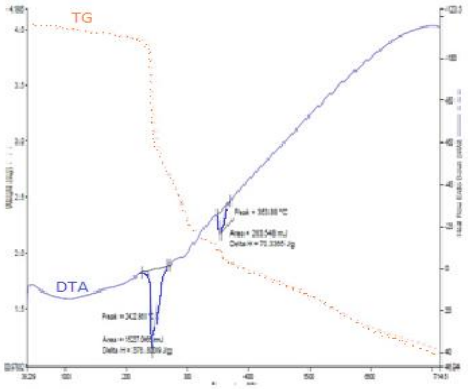

e)

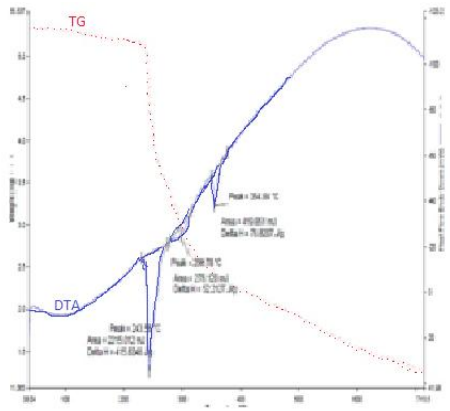

h)

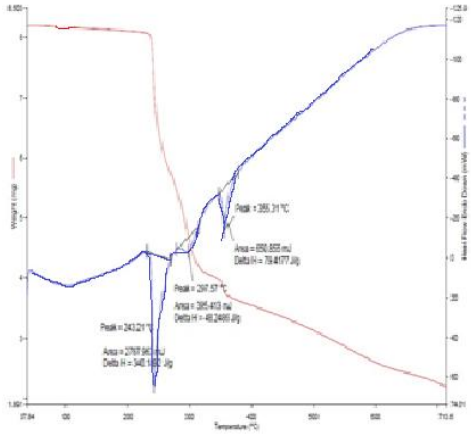

i)

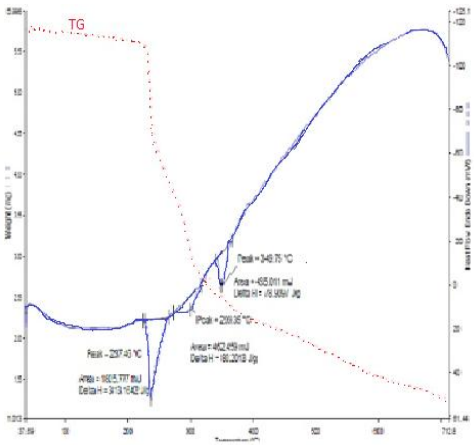

j)

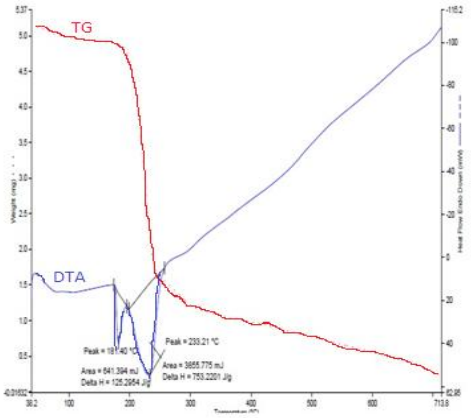

k)

3.8 Density studies

The density of ZTS crystal was found to be 1.927g/cm^{3}and it is in good agreement with the literature values (1.923g/cm3 [25]). The density of MTS was found to be 2.097g/cm^3. The change of density also indicates the incorporation of impurity in the ZTS crystal. The density was also calculated from the Single crystal XRD data using the relation $\rho = (M.Z)/(N.V)$, where M is the molecular weight of the ZTS crystal, Z is the number of molecules per unit cell, N is Avagadro's number, and V is the volume of the unit cell. The values are shown in Table 8.

Table 8: Density values of ZMTS crystals

Sample	**Density** by floatation method (g/cc)	**Density** by SXRD (g/cc)
ZTS	1.927	1.931
ZTS9	1.923	1.911
ZTS8	1.921	1.892
ZTS7	1.930	1.878
ZTS6	1.933	1.846
ZTS5	1.939	1.827
ZTS4	1.945	1.819
ZTS3	1.950	1.788
ZTS2	1.962	1.763
ZTS1	1.975	1.769
MTS	2.09	1.977

IV. Conclusions

Single crystals of ZMTS crystals were grown by the aqueous solution method with the slow evaporation technique at room temperature. Unit cell parameters of the ZMTS crystals were found by single crystal XRD analysis. Sharp peaks of powder XRD spectrum of the crystal show good crystalline nature of the compound. The presence of various functional groups was confirmed by FT-IR analysis. UV-Visible study shows that the grown crystal has wide range of transparency in UV and entire visible region and cutoff wave length of ZTS is around 290 nm. The Vicker's micro hardness was calculated in order to understand the mechanical stability of the grown crystals. Hardness measurement also shows that ZMTS crystals are soft materials. TGA analysis of MTS shows that the grown crystal has very good thermal stability up to 181.40°C. Thus the Magnesium added ZTS crystal is going to play vital role in the field of optoelectronics and laser technology. The SHG efficiency was found to be 0.78 times that of KDP. It confirms the NLO property of the grown ZMTS crystals. Density of the grown crystals was measured by the floatation method and it was observed to be in good agreement with the crystallographic data.

References

[1]. Aggarwal, M.D., choi, J., Wang, W.S., Bhat,K., Lal,R.B., Shield, A.D., Penn, B.G., Frazier,D.O, J.Crystalgrowth 204(1999)179.
[2]. R. Rajasekaran, R. Mohankumar, R.Jayavel, P. Ramasamy, J.Cryst.growth 252(2002) 317.
[3]. P.RNewman, L.F.Warran, P.Cunningham, T.V. Chang, D.E .Cooper, G.L Burdge, P.P. Dingels, C. K. Lowema, Mater. Res. Soc. Symp. Proc.173 (1990) 557.
[4]. V. Venkataramanan, G.Dhanaraj, V. K. Wadhawan, J.NSherwood, H.Lrowth 154 (1995)92.
[5]. Selvasekarapandian S., Vivekanandian K., Kolandaivel P., and Gundurao T. K., 1997, "Vibrational Studies of Bis(thiourea) Cadmium Chloride and Tris(thiourea) Zinc Sulphate Semiorganic Non-linear Optical Crystals", Cryst. Res. Technol. 32, pp. 299-309.
[6]. Elmert,D., Velsko,S., Davis,L., Wang,F., Loiaceono,G., Kennedy,G.IEEE.J.Quantum Electron. 25 (1989)179.
[7]. Hellwege, K.H.,Hellwage, A.M.Landott – Bornstein Group II 14 (1982) 584.
[8]. G. Pasupathy, P. Philominathan, *Modern Phy. Lett*. 23B, **2009**, 3035-3043.
[9]. Xing,G., Jiang,M., Shao,Z., Xu,D. Chin.phys.Lasers 14 (1987) 357.
[10]. Ushasree P, Muralidharan M, Jeyavel R, Ramasamy P. J Cryst Growth 2000; 210: 741–5.
[11]. Anie Roshan,S., Joseph,C., Ittachen, M.A Matter.Lett. 49 (2001) 299.
[12]. Meera,K., Muralidharan,R., Dhanasekaran,R., Prapun Manyum, Ramasamy,P.J.Cryst.Growth 263 (2004) 510.
[13]. Pricilla Jeyakumari,A., Ramajothi,J., Dhanuskodi,S., J.Cryst.Growth 269 (2004) 558.
[14]. Rajasekaran,R., Ushasree,P.M., Jayavel,R., Ramasamy,P. J.Cryst.Growth 229(2001) 563.
[15]. Ramajothi,J., Dhanuskodi,S., Nagarajan,K., Cryst.Res. Technol. 39 (2004) 414.
[16]. Ushasree, P.M., Muralidharan,R., Jayavel,R., Ramasamy,P. J.Cryst.Growth 210 (2000) 741.
[17]. M.Oussaid, P.Becker, M.Kemiche, C.Carabates-Nedelec, Phys.Stat.Sol. B 207 (1998) 103.
[18]. Dhumane V.G,N.R., Hussaini, S.S., Dongre, V.G., Mahendra, Shirsat,D. Optical Materials, Volume 31, Issue2, October – December 2008, Pages 328-332.
[19]. Gupte sonal S. Pradhan Ranjit D.J Appl Phys 2002; 91:3125-8.
[20]. Krishnan,C., Selvarajan,P., Freeda,T.H., Mahadevan,C.K. Physica B: Condensed Matter, Volume 404, Issue 2, 28 February 2009, and Pages 289 – 294.
[21]. Venkataramanan V., Subramanian C.K., Bhat H.L. J.App. Phys 1995; 77: 6049-51.
[22]. Krishnan,C., Selvarajan,P., Freeda,T.H. Materials and Manu. Proces. 23:800-804, 2008.
[23]. G.D. Andreeti, L.Cavalca,A. Musatti, Acta Crystallogr.Sect.B 24 (1968) 683.
[24]. H.Lipson, H.Steeple, Interpretation of X-ray powder Diffraction Patterns, fifth ed., Macmillan, New York, 1970.
[25]. V.Venkatramanan,Ph.D. Thesis, Indian Institute of Science, Bangalore, India, 1994.
[26]. G.D. Andreeti, L.Cavalca, A.Musatti, Acta Crystallogr. Sect. B 24 (1968) 683.
[27]. C.Krishnan, P.Selvarajan, T.H. Freeda, C.K. Mahadevan, Physica B404 (2009) 289-294.
[28]. A.Ruby, S.Alfred Cecil Raj, Archives of Physics Research, 2012, 3 (2):130-137
[29]. R. Ramjothi, S. Dhanushkodi, K. Nagarajan, *Cryst. Res. Technol*. 39 **2004**, 414
[30]. Kurtz, S.K., Perry, T.T., J. Appl. Phys., 39 (1968) 3798-3813.
[31] K. Kishan Rao, V. Surender, B. Sabitha Rani, Bull. Mater. Sci. **25**, (2002).
[32] E. M. Onitsch, Mikroskopic, **2**, 131 (1947) [31] B. W. Mott, Micro Indentation Hardness Testing, Butterworth, London, 1956
[33] J. Ramajothi, S. Dhanuskodi, K. Nagarajan, Cryst.Res. Technol. **39**, 414 (2004).
[34]. K. Kanagasabapathy, R. Rajasekaran, Optoelectronics and Advanced Materials – RAPID Communications Vol. 6, 2012, p. 218 – 224
[35]. N.R. Dhumane, S.S. Hussaini, Kunal Datta, Prasanta Ghosh and Mahendra D. Shirsat**,** Recent Research in Science and Technology 2010, 2(10): 30-34
[36] C.Krishnan, P.Selvarajan, journal of Experimental Sciences Vol.1,Issue3,Pages 23-26[2010].
[37] Charles Kittle, Introduction to solid state physics,seventh ed., Wiley India Edition, New Delhi,2007.